ISSN 1392 - 1207. MECHANIKA. 2012 Volume 18(5): 508-516

Complete closed-form solution for pressurized heterogeneous thick spherical shells

Mehdi Ghannad*, Mohammad Zamani Nejad**
**Mechanical Engineering Faculty, Shahrood University of Technology, Shahrood, Iran*
E-mail: ghannad.mehdi@gmail.com
***Mechanical Engineering Department, Yasouj University, Yasouj P. O. Box: 75914-353, Iran*
E-mail: m.zamani.n@gmail.com

crossref http://dx.doi.org/10.5755/j01.mech.18.5.2702

1. Introduction

A thick-walled spherical shell subjected to pressure in radial direction is one of the classical problems in engineering mechanics. This problem was studied by several researchers in the past. Among them, Timoshenko and Goodier [1] obtained the analytical expressions of stresses and displacement in a thick-walled sphere subjected to internal and external pressure. In the recent past, there has been a strong increase in the interest in functionally graded materials. FGMs are composite materials that are microscopically nonhomogeneous but at macrolevel, the mechanical properties vary continuously from one surface to another by smoothly varying the volume fractions of the material constituents. Heterogeneous composite materials are FGMs with gradient compositional variation of the constituents from one surface of the material to the other which results in continuously varying material properties. These materials are advanced, heat resisting, erosion and corrosion resistant, and have high fracture toughness. The FGM spherical shells are widely used in many engineering fields such as aerospace, mechanical, naval, nuclear energy, chemical plant, electronics, and biomaterials and so on.

Closed-form solutions are obtained by Tutuncu and Ozturk [2] for cylindrical and spherical vessels with variable elastic properties obeying a simple power law through the wall thickness which resulted in simple Euler-Cauchy equations whose solutions were readily available Elastic analysis of internally pressurized thick-walled spherical pressure vessels of functionally graded materials was studied [3]. In the paper, two kinds of pressure vessels are considered: one consists of two homogeneous layers near the inner and outer surfaces of the vessel and one functionally graded layer in the middle; the other consists of the functionally graded material only. Based on the assumption that Poisson's ratio is constant and modulus of elasticity is an exponential function of radius, Chen and Lin [4] have analyzed stresses and displacements in FG cylindrical and spherical pressure vessels. A hollow sphere made of FGMs subjected to radial pressure was analyzed in [5]. Using plane elasticity theory and Complementary Functions method, Tutuncu and Temel [6] obtained axisymmetric displacements and stresses in functionally-graded hollow cylinders, disks and spheres subjected to uniform internal pressure. Zamani Nejad et al. [7] developed 3-D set of field equations of FGM thick shells of revolution in curvilinear coordinate system by tensor calculus. Deformations and stresses inside multilayered thick-walled spheres are investigated [8]. In the paper, each sphere is characterized by its elastic modules. Assuming the volume fractions of two phases of a FG material (FGM) vary only with the radius, Nie et. al. [9] obtained a technique to tailor materials for functionally graded (FG) linear elastic hollow cylinders and spheres to attain through the thickness either a constant hoop (or circumferential) stress or a constant in-plane shear stress.

In this study, a complete analytical solution for FGM thick-walled spherical shells subjected to internal and/or external pressures is presented. The analytical solution which is closed-form is obtained for real, double and complex roots of equation and distribution of stresses and displacement are compared with the solution using finite element method.

2. Basic formulations of the problem

Consider a thick hollow FGM sphere with an inner radius R_i, and an outer radius R_o, subjected to internal and external pressure P_i and P_o, respectively.

The classical theory is based on the assumption that the straight sections perpendicular to the central axis of the sphere remains unchanged after loading and deformation. According to this theory, the deformations are axisymmetric and do not change along the circumference of sphere. In other words, the radial deformation is dependent only on radius $u_R(R)$. The value of shear strains and shear stresses are zero. Therefore, normal stresses are principal stresses. In the spherical shells, because of dual central symmetry, both the values of circumferential and meridional strains and those of stresses are equal. Thus,

$$\left.\begin{aligned}\varepsilon_\varphi &= \varepsilon_\theta \\ \sigma_\varphi &= \sigma_\theta\end{aligned}\right\} \tag{1}$$

The strains are expressed in terms of the radial displacement u_R as follows

$$\left.\begin{aligned}\varepsilon_R &= \frac{du_R}{dR} \\ \varepsilon_\varphi = \varepsilon_\theta &= \frac{u_R}{R}\end{aligned}\right\} \tag{2}$$

The equilibrium equation of the FGM hollow sphere, in absence of body forces, is expressed as

$$\frac{d\sigma_R}{dR}+\frac{1}{R}\left(2\sigma_R-\sigma_\theta-\sigma_\varphi\right)=0 \tag{3}$$

and the constitutive relations for nonhomogenous and isotropic materials are

$$\begin{Bmatrix}\sigma_R\\ \sigma_\theta\\ \sigma_\varphi\end{Bmatrix}=E(R)\begin{bmatrix}A & B & B\\ B & A & B\\ B & B & A\end{bmatrix}\begin{Bmatrix}\varepsilon_R\\ \varepsilon_\theta\\ \varepsilon_\varphi\end{Bmatrix} \tag{4}$$

A and B are related to Poisson's ratio, $(\upsilon=const.)$ as

$$A=\frac{1-\upsilon}{(1+\upsilon)(1-2\upsilon)},\ B=\frac{\upsilon}{(1+\upsilon)(1-2\upsilon)} \tag{5}$$

It is assumed that the nonhomogeneous modulus of elasticity E is power function of R as

$$E(R)=E_i\left(\frac{R}{R_i}\right)^n \tag{6}$$

where E_i is the modulus of elasticity at the internal surface $R = R_i$, and n is the inhomogeneous constant determined empirically.

Now suppose that $r=R/R_i$, thus Eqs. (2) to (4) and (6) may be rewritten as

$$\varepsilon_R=\frac{du_r}{dr},\ \varepsilon_\varphi=\varepsilon_\theta=\frac{u_r}{r} \tag{7}$$

$$\frac{d\sigma_R}{dr}+\frac{2}{r}\left(\sigma_R-\sigma_\varphi\right)=0 \tag{8}$$

$$\begin{Bmatrix}\sigma_R\\ \sigma_\varphi\end{Bmatrix}=E(r)\begin{bmatrix}A & 2B\\ B & A+B\end{bmatrix}\begin{Bmatrix}\varepsilon_R\\ \varepsilon_\varphi\end{Bmatrix} \tag{9}$$

$$E(r)=E_i r^n \tag{10}$$

Substitution of Eqs. (7) and (10) into Eq. (9), and the use of Eq. (8) lead to the equation

$$\frac{d}{dr}\left[E(r)\left(A\frac{du_r}{dr}+2B\frac{u_r}{r}\right)\right]+ +\frac{2}{r}\left[E(r)(A-B)\left(\frac{du_r}{dr}-\frac{u_r}{r}\right)\right]=0 \tag{11}$$

After simplification, Eq. (11) is expressed as

$$\frac{d^2u_r}{dr^2}+\left(\frac{n+2}{r}\right)\frac{du_r}{dr}+\frac{2}{r^2}\left(n\frac{B}{A}-1\right)u_r=0 \tag{12}$$

Eq. (12) is the nonhomogeneous Euler-Caushy equation

$$r^2u_r''+(n+2)ru_r'+\left(n\upsilon^*-1\right)u_r=0 \tag{13}$$

where $'$ and $''$ denote first and second differentiation with respect to r and the value of $\upsilon^*=B/A$ is obtained based on Eq. (5).

Substituting $u_r(r)=r^m$ in Eq. (13), the characteristic equation is obtained as follows

$$m^2+(n+1)m+2\left(n\upsilon^*-1\right)=0 \tag{14}$$

The roots of characteristic equation are

$$\left.\begin{aligned}m_{1,2}&=-\frac{n+1}{2}\pm\frac{\sqrt{\Delta}}{2}\\ \Delta&=n^2+2\left(1-4\upsilon^*\right)n+9\end{aligned}\right\} \tag{15}$$

These roots may be (i) real, (ii) double, (iii) complex.

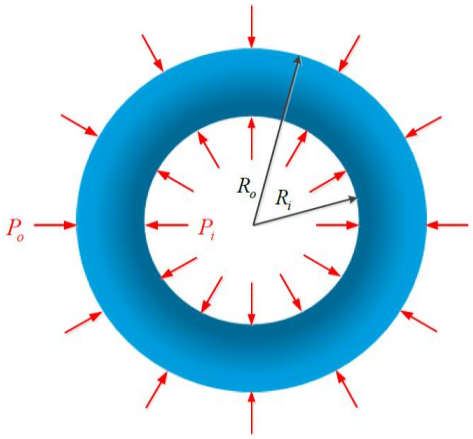

Fig. 1 Cross-section of heterogeneous thick sphere

3. Solution for heterogeneous thick sphere

Now, differential Eq. (13) for real, double and complex roots will be solved. Following that, in each of the cases, parametric equations of radial stress, meridional stress and radial displacement will be derived.

3.1. Real roots

In this case, $\Delta>0$ and we have

$$\left.\begin{aligned}m_1&=-\frac{n+1}{2}+\frac{\sqrt{\Delta}}{2}\quad,\quad m_2=-\frac{n+1}{2}-\frac{\sqrt{\Delta}}{2}\\ \Delta&=n^2+2\left(1-4\upsilon^*\right)n+9\end{aligned}\right\} \tag{16}$$

The solution of Eq. (13) is as follows

$$u_r(r)=C_1r^{m_1}+C_2r^{m_2} \tag{17}$$

With substitution of Eqs. (17) into Eq. (7) and then use of Eq. (9), radial and meridional stresses are obtained as follows

$$\sigma_R=E_ir^{n-1}\begin{bmatrix}C_1(Am_1+2B)r^{m_1}+\\ +C_2(Am_2+2B)r^{m_2}\end{bmatrix} \tag{18}$$

$$\sigma_\varphi=E_ir^{n-1}\begin{bmatrix}C_1(Bm_1+(A+B))r^{m_1}+\\ +C_2(Bm_2+(A+B))r^{m_2}\end{bmatrix} \tag{19}$$

For a sphere subjected to internal and external pressure, constants C_1 and C_2 are determined using boundary conditions as

$$\sigma_R\Big|_{r=1} = -P_i \quad , \quad \sigma_R\Big|_{r=k} = -P_o \tag{20}$$

thus

$$\left.\begin{aligned} C_1 &= \frac{k^{m_2}P_i - k^{1-n}P_o}{E_i\left(Am_1+2B\right)\left(k^{m_1}-k^{m_2}\right)} \\ C_2 &= \frac{-k^{m_1}P_i + k^{1-n}P_o}{E_i\left(Am_2+2B\right)\left(k^{m_1}-k^{m_2}\right)} \end{aligned}\right\} \tag{21}$$

where $k = R_o/R_i$.

With substituting C_1 and C_2 into Eqs. (17) and (9), σ_R , σ_φ and u_R are obtained as follows

$$\sigma_R = \frac{r^{n-1}}{k^{m_1}-k^{m_2}}\left[\left(k^{m_2}P_i - k^{1-n}P_o\right)r^{m_1} - \left(k^{m_1}P_i - k^{1-n}P_o\right)r^{m_2}\right] \tag{22}$$

$$\sigma_\varphi = \frac{r^{n-1}}{k^{m_1}-k^{m_2}}\left[\frac{(A+B)+Bm_1}{Am_1+2B}\left(k^{m_2}P_i - k^{1-n}P_o\right)r^{m_1} - \frac{(A+B)+Bm_2}{Am_2+2B}\left(k^{m_1}P_i - k^{1-n}P_o\right)r^{m_2}\right] \tag{23}$$

$$u_R = \frac{R_i}{E_i\left(k^{m_1}-k^{m_2}\right)}\left[\frac{1}{Am_1+2B}\left(k^{m_2}P_i - k^{1-n}P_o\right)r^{m_1} - \frac{1}{Am_2+2B}\left(k^{m_1}P_i - k^{1-n}P_o\right)r^{m_2}\right] \tag{24}$$

Now, given the Eq. (5), Eqs. (23) and (24) may be rewritten as follows

$$\sigma_\varphi = \frac{r^{n-1}}{k^{m_1}-k^{m_2}}\left[\frac{1+\upsilon m_1}{(1-\upsilon)m_1+2\upsilon}\left(k^{m_2}P_i - k^{1-n}P_o\right)r^{m_1} - \frac{1+\upsilon m_2}{(1-\upsilon)m_2+2\upsilon}\left(k^{m_1}P_i - k^{1-n}P_o\right)r^{m_2}\right] \tag{25}$$

$$u_R = \frac{(1+\upsilon)(1-2\upsilon)R_i}{E_i\left(k^{m_1}-k^{m_2}\right)}\left[\frac{1}{(1-\upsilon)m_1+2\upsilon}\left(k^{m_2}P_i - k^{1-n}P_o\right)r^{m_1} - \frac{1}{(1-\upsilon)m_2+2\upsilon}\left(k^{m_1}P_i - k^{1-n}P_o\right)r^{m_2}\right] \tag{26}$$

The value of effective stress based on von Mises and Tresca failure theories is as follows

$$\sigma_{eff} = \left|\sigma_R - \sigma_\varphi\right| = \left|\frac{r^{n-1}}{k^{m_1}-k^{m_2}}\left[\frac{(1-2\upsilon)(m_1-1)}{(1-\upsilon)m_1+2\upsilon}\left(k^{m_2}P_i - k^{1-n}P_o\right)r^{m_1} - \frac{(1-2\upsilon)(m_2-1)}{(1-\upsilon)m_2+2\upsilon}\left(k^{m_1}P_i - k^{1-n}P_o\right)r^{m_2}\right]\right| \tag{27}$$

In [2], radial and meridional stresses are obtained only for $\Delta > 0$ case. The equation of radial stress has been obtained correctly while the equation of meridional stress has been derived incorrectly.

$$m_1 = m_2 = m = -\frac{n+1}{2} \tag{28}$$

In this case, the solution of Eq. (13) is as follows.

$$u_r(r) = \left(C_1 + C_2 \ln r\right)r^m \tag{29}$$

With substitution of Eq. (29) into Eq. (7) and then use of Eq. (9), radial and meridional stresses are obtained as follows

$$\sigma_R = E_i r^{n+m-1}\left\{C_1\left(Am+2B\right) + C_2\left[A + \left(Am+2B\right)\ln r\right]\right\} \tag{30}$$

$$\sigma_\varphi = E_i r^{n+m-1}\left\{C_1\left(Bm+A+B\right) + C_2\left[B + \left(Bm+A+B\right)\ln r\right]\right\} \tag{31}$$

To determine the unknown constants C_1 and C_2, using boundary conditions (20), yields

$$\left.\begin{aligned} C_1 &= -\frac{\left[A + \left(Am+2B\right)\ln k\right]P_i + Ak^{1-m-n}P_o}{E_i\left(Am+2B\right)^2 \ln k} \\ C_2 &= \frac{\left[P_i - k^{1-m-n}P_o\right]}{E_i\left(Am+2B\right)\ln k} \end{aligned}\right\} \tag{32}$$

With substituting C_1 and C_2 into Eqs. (29) to (31), σ_R , σ_φ and u_R are obtained as follows

$$\sigma_R = -\frac{r^{n+m-1}}{\ln k}\left[P_i \ln\frac{k}{r} + k^{1-m-n}P_o \ln r\right] \tag{33}$$

3.2. Double roots

In Eq. (15), if $\Delta = 0$, then the equation will have double roots.

$$\sigma_{\varphi}=\frac{r^{n+m-1}}{\ln k}\left\{\frac{2B^2-A^2-AB}{(Am+2B)^2}\left[P_i-k^{1-m-n}P_o\right]-\frac{Bm+A+B}{Am+2B}\left[P_i\ln\frac{k}{r}+k^{1-m-n}P_o\ln r\right]\right\} \tag{34}$$

$$u_R=-\frac{R_i r^m}{E_i(Am+2B)\ln k}\left\{\frac{A}{Am+2B}\left[P_i-k^{1-m-n}P_o\right]+\left[P_i\ln\frac{k}{r}+k^{1-m-n}P_o\ln r\right]\right\} \tag{35}$$

Given the Eq. (5), Eqs. (34) and (35) may be rewritten as follows

$$\sigma_{\varphi}=-\frac{r^{n+m-1}}{\ln k}\left\{\frac{(1+\upsilon)(1-2\upsilon)}{\left[(1-\upsilon)m+2\upsilon\right]^2}\left[P_i-k^{1-m-n}P_o\right]+\frac{1+\upsilon m}{(1-\upsilon)m+2\upsilon}\left[P_i\ln\frac{k}{r}+k^{1-m-n}P_o\ln r\right]\right\} \tag{36}$$

$$u_R=-\frac{(1+\upsilon)(1-2\upsilon)R_i r^m}{E_i\left[(1-\upsilon)m+2\upsilon\right]\ln k}\left\{\frac{1-\upsilon}{(1-\upsilon)m+2\upsilon}\left[P_i-k^{1-m-n}P_o\right]+\left[P_i\ln\frac{k}{r}+k^{1-m-n}P_o\ln r\right]\right\} \tag{37}$$

3.3. Complex roots

In Eq. (15), if $\Delta<0$, then the equation will have complex roots.

$$\left.\begin{aligned}&m_1=z+iy,\ m_2=z-iy\\&z=-\frac{n+1}{2},\ y=\frac{\sqrt{-\Delta}}{2}\\&\Delta=n^2+2\left(1-4\upsilon^*\right)n+9\end{aligned}\right\} \tag{38}$$

In this case, the solution of Eq. (13) is as follows

$$u_r(r)=\left[C_1\cos(y\ln r)+C_2\sin(y\ln r)\right]r^z \tag{39}$$

With the substitution of Eq. (39) into Eq. (7) and then use of Eq. (9), radial and meridional stresses are obtained as follows

$$\sigma_R=E_i r^{n+z-1}\left\{C_1\left[(Az+2B)\cos(y\ln r)-Ay\sin(y\ln r)\right]+C_2\left[(Az+2B)\sin(y\ln r)+Ay\cos(y\ln r)\right]\right\} \tag{40}$$

$$\sigma_{\varphi}=E_i r^{n+z-1}\left\{C_1\left[(Az+2B)\cos(y\ln r)-Ay\sin(y\ln r)\right]+C_2\left[(Az+2B)\sin(y\ln r)+Ay\cos(y\ln r)\right]\right\} \tag{41}$$

Using boundary conditions (20), constants C_1 and C_2 are obtained as follows

$$\left.\begin{aligned}C_1&=\frac{-1}{E_i D\sin(y\ln k)}\left\{\left[(Az+2B)\sin(y\ln k)+Ay\cos(y\ln k)\right]P_i-AyP_o k^{1-n-z}\right\}\\C_2&=\frac{1}{E_i D\sin(y\ln k)}\left\{\left[(Az+2B)\cos(y\ln k)-Ay\sin(y\ln k)\right]P_i-(Az+2B)P_o k^{1-n-z}\right\}\end{aligned}\right\} \tag{42}$$

where

$$D=\left[(Az+2B)^2+A^2y^2\right] \tag{43}$$

With substituting C_1 and C_2 into Eq. (39) to (41), σ_R, σ_{φ} and u_R are obtained as follows

$$\sigma_R=-\frac{r^{n+z-1}}{\sin(y\ln k)}\left[\sin\left(y\ln\frac{k}{r}\right)P_i+\sin(y\ln r)P_o k^{1-n-z}\right] \tag{44}$$

$$\sigma_{\varphi}=-\frac{r^{n+z-1}}{D\sin(y\ln k)}\left\{\begin{aligned}&\left[(Az+2B)(Bz+A+B)+ABy^2\right]\left[\sin\left(y\ln\frac{k}{r}\right)P_i+\sin(y\ln r)P_o k^{1-n-z}\right]+\\&+\left(A^2+AB-2B^2\right)y\left[\cos\left(y\ln\frac{k}{r}\right)P-\cos(y\ln r)P_o k^{1-n-z}\right]\end{aligned}\right\} \tag{45}$$

$$u_R=\frac{R_i r^z}{E_i D\sin(y\ln k)}\left\{(Az+2B)\left[\sin\left(y\ln\frac{k}{r}\right)P_i+\sin(y\ln r)P_o k^{1-n-z}\right]+Ay\left[\cos\left(y\ln\frac{k}{r}\right)P_i-\cos(y\ln r)P_o k^{1-n-z}\right]\right\} \tag{46}$$

Given the Eqs. (5), (45) and (46) may be rewritten as follows

$$\sigma_{\varphi}=-\frac{r^{n+z-1}}{D\sin(y\ln k)}\left\{\begin{array}{l}\left[\left[(1-\upsilon)z+2\upsilon\right](1+\upsilon z)+\upsilon(1-\upsilon)y^{2}\right]\left[\sin\left(y\ln\frac{k}{r}\right)P_i+\sin(y\ln r)P_o k^{1-n-z}\right]+\\ +(1+\upsilon)(1-2\upsilon)y\left[\cos\left(y\ln\frac{k}{r}\right)P_i-\cos(y\ln r)P_o k^{1-n-z}\right]\end{array}\right\} \tag{47}$$

$$u_R=-\frac{(1+\upsilon)(1-2\upsilon)R_i r^{z}}{E_i D\sin(y\ln k)}\left\{\begin{array}{l}\left[(1-\upsilon)z+2\upsilon\right]\left[P_i\sin\left(y\ln\frac{k}{\bar{r}}\right)+k^{1-z-n}P_o\sin(y\ln\bar{r})\right]+\\ +(1-\upsilon)y\left[P_i\cos\left(y\ln\frac{k}{\bar{r}}\right)-k^{1-z-n}P_o\cos(y\ln\bar{r})\right]\end{array}\right\} \tag{48}$$

where

$$D=\left[(1-\upsilon)z+2\upsilon\right]^{2}+\left[(1-\upsilon)y\right]^{2} \tag{49}$$

4. Solution for thick homogenous spheres

In thick homogenous and isotropic spheres, modulus of elasticity and Poisson's ratio are both constant. By substituting $n = 0$ into Eq. (6), homogenous materials are obtained. In this case, Euler-Caushy equation (Eq. (13)) in terms of the displacement is as

$$r^{2}u_r''+2ru_r'-2u_r=0 \tag{50}$$

The characteristic equation and the roots of characteristic equation are as follows:

$$m^{2}+m-2=0 \quad\Rightarrow\quad m_{1,2}=+1,-2 \tag{51}$$

It could be observed that roots of the characteristic equation are the real (roots are in set of $\Delta > 0$).

$$u_r(r)=C_1 r+\frac{C_2}{r^{2}} \tag{52}$$

Using the boundary conditions are given in Eq. (20), the constants of C_1 and C_2 become

$$\left.\begin{array}{l}C_1=\dfrac{P_i-k^{3}P_o}{E(A+2B)(k^{3}-1)}\\ C_2=\dfrac{k^{3}(P_i-P_o)}{2E(A-B)(k^{3}-1)}\end{array}\right\} \tag{53}$$

Substituting C_1 and C_2 in Eq. (52) and using Eqs. (7) and (9). Thus

$$\sigma_R^{H}=\frac{1}{k^{3}-1}\left[\left(P_i-k^{3}P_o\right)-\left(P_i-P_o\right)\frac{k^{3}}{r^{3}}\right] \tag{54}$$

$$\sigma_{\varphi}^{H}=\frac{1}{k^{3}-1}\left[\left(P_i-k^{3}P_o\right)+\left(P_i-P_o\right)\frac{k^{3}}{2r^{3}}\right] \tag{55}$$

$$u_R^{H}=\frac{R_i r}{E\left(k^{3}-1\right)}\left[\left(\frac{P_i-k^{3}P_o}{A+2B}\right)+\left(\frac{P_i-P_o}{A-B}\right)\frac{k^{3}}{2r^{3}}\right] \tag{56}$$

The values of the radial and meridional stresses in homogeneous and isotropic thick-walled spheres subjected to constant pressure, with the same dimensions and different values of modulus of elasticity are equal.

The value of effective stress based on von Mises and Tresca failure theories is as follows

$$\sigma_{eff}^{H}=\frac{3}{2\left(k^{3}-1\right)}\left|\left(P_i-P_o\right)\frac{k^{3}}{r^{3}}\right| \tag{57}$$

Radial displacement (Eq. (56)) may be rewritten as follows

$$u_R^{H}=\frac{R_i r}{E\left(k^{3}-1\right)}\left[\begin{array}{l}(1-2\upsilon)\left(P_i-k^{3}P_o\right)+\\ +(1+\upsilon)\left(P_i-P_o\right)\dfrac{k^{3}}{2r^{3}}\end{array}\right]. \tag{58}$$

5. Results and discussion

Consider a heterogeneous thick-walled sphere, subjected to internal and/or external constant uniform pressures of 80 MPa, with the internal radius of $R_i = 40$ mm and the outer radius of $R_o = 60$ mm. The modulus of elasticity E_i at internal radius has the value of 200 GPa. It is also assumed that the Poisson's ratio, υ, has a constant value of 0.3.

5.1. Homogeneous sphere

Radial and meridional stresses in homogeneous and isotropic spheres are independent of the mechanical properties; whereas, radial displacement is dependent on mechanical properties. Figs. 2 to 4 are plotted according to the internal pressure $P_i = 80$ MPa and/or external pressure $P_o = 80$ MPa.

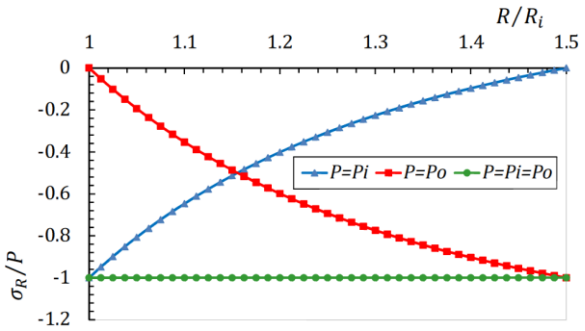

Fig. 2 Distribution of radial stress, $P = 80$ MPa (homogeneous sphere)

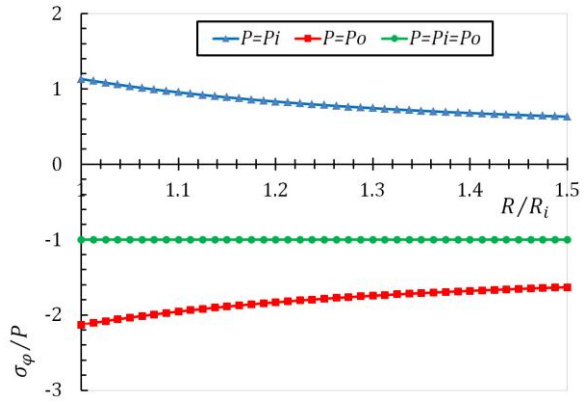

Fig. 3 Distribution of meridional stress, P = 80 MPa (homogeneous sphere)

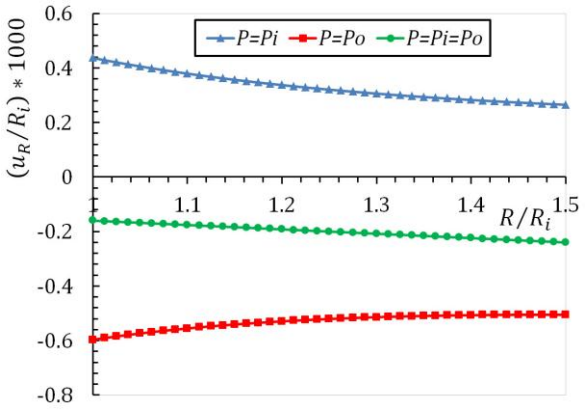

Fig. 4 Distribution of radial displacement, P = 80 MPa (homogeneous sphere)

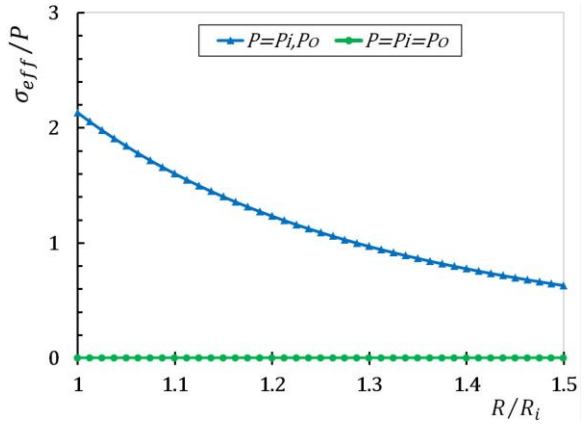

Fig. 5 Distribution of effective stress, P = 80 MPa (homogeneous sphere)

Distribution of compressive radial stress based on Eq. (54) is shown in Fig. 2. When both the internal and external pressures are applied, and their values are equal, the radial stress will be constant along the wall.

In Fig. 3, distribution of meridional stress based on Eq. (55) is shown. Along the wall, the meridional stress will be tensile while just the internal pressure is present; whereas, it will be compressive when just the external pressure is there. When the internal and external pressures are equal, the meridional stress will be compressive and constant in value along the wall. The meridional stress is more in the case of external pressure compared to that of the other two cases. In Fig. 4, distribution of radial displacement based on Eq. (56) is shown. In the case where only the internal pressure is present, the radial displacement is expansionary; whereas, in other two cases it is contractionary. The highest value of radial displacement occurs in the case of the external pressure. Distribution of effective stress based on Eq. (57) is shown in Fig. (5). It is observed that, when $P_i = P_o$, the value of effective stress for homogeneous sphere is equal to zero.

5.2. Heterogeneous sphere

In nonhomogeneous and isotropic spheres, radial and meridional stresses are dependent on mechanical properties by means of n; while radial displacement depends on them by means of both n and E_i. Modulus of elasticity through the wall thickness is assumed to vary as $E(R) = E_i(R/R_i)^n$ in which the range $-2 \le n \le 2$ is used in the present study.

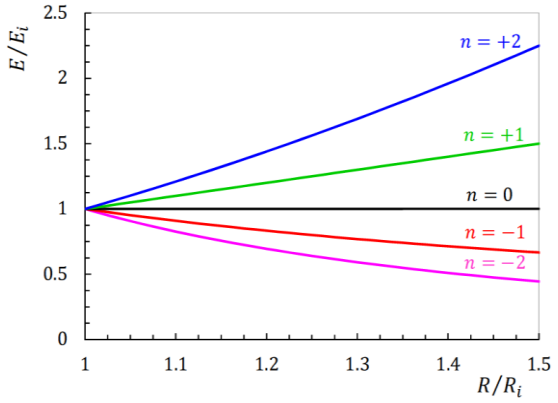

Fig. 6 Distribution of modulus of elasticity

In Fig. 6, for different values of n modulus of elasticity along the radial direction is plotted. It is apparent from the curve that a positive n means increasing stiffness in the radial direction whereas a negative value of n results in a decrease in stiffness in the radial direction.

5.2.1. Internal pressure

Here the nonhomogeneous sphere is only under internal pressure, P_i = 80 MPa.

Fig. 7 shows the distribution of the compressive radial stress along the radius. The value of stress in inner and outer layers is the same, and for both layers σ_R / σ_R^H is one. Along the radius, for $n < 0$, the radial stress decreases whereas for $n > 0$ the radial stress increases. The decrease and increase of the stress depend on $|n|$.

Fig. 8 shows the distribution of the tensile meridional stress along the radius. The value of stress in inner and outer layers is not the same, and for both layers $\sigma_\varphi / \sigma_\varphi^H$ is not one. The value of the meridional stress is more than the homogeneous material for $n < 0$ in the inner half of the wall thickness while it is less than that in the outer half. This will be reverse, where $n > 0$. The curve associated with $n = 1$ shows that the variation of meridional stress along the radial direction is minor and is almost constant across the radius which can be an advantage in terms of stress control. It is observed that in the range of the inner layer of the sphere, the graphs converge and behave similarly.

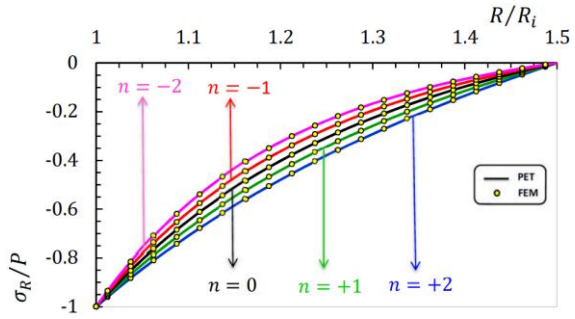

Fig. 7 Distribution of radial stress, P_i = 80 MPa (heterogeneous sphere)

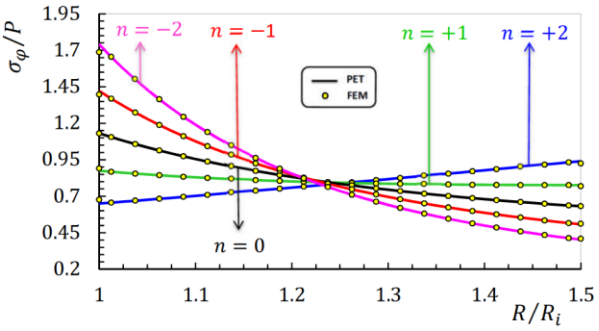

Fig. 8 Distribution of meridional stress, P_i = 80 MPa (heterogeneous sphere)

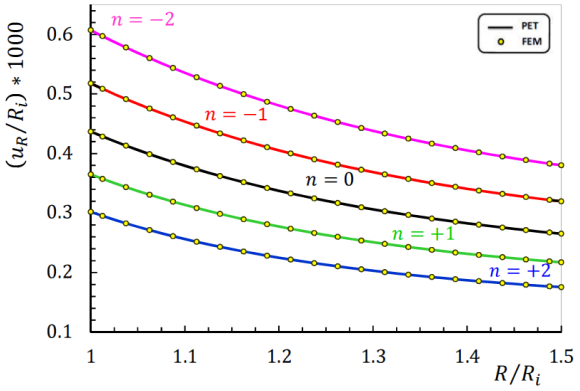

Fig. 9 Distribution of radial displacement, P_i = 80 MPa (heterogeneous sphere)

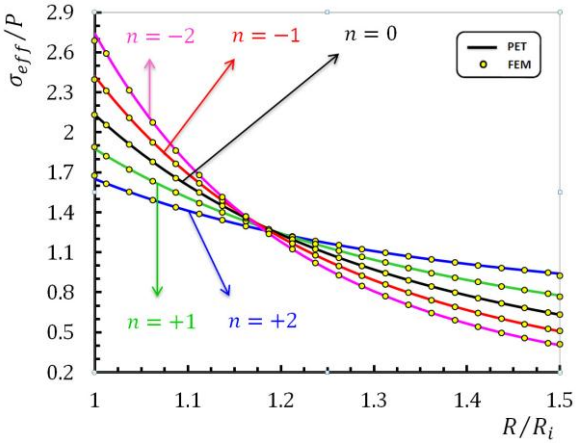

Fig. 10 Distribution of effective stress, P_i = 80 MPa (heterogeneous sphere)

Fig. 9 shows the distribution of the radial displacement of the sphere along the radius. u_R / u_R^H is not one at any point. For $n < 0$ the radial displacement of the sphere is more than where the material is homogeneous and it is the reverse for $n > 0$. Yet this ratio remains almost constant along the wall thickness.

The graph of effective stress based on Eq. (27) is shown in Fig. 10. It must be noted from this figure that at the same position, almost for $(R/R_i) < 1.18$, there is a decrease in the value of the effective stress as n increases, whereas for $(R/R_i) > 1.18$ this situation was reversed.

5.2.2. External pressure

In this section, the nonhomogeneous sphere is only under external pressure, $P_o = P$ = 80 MPa.

The distribution of the compressive radial stress of the sphere along the radius is shown in Fig. 11. The value of the stress in the inner and outer layers of the sphere is the same and $\sigma_R / \sigma_R^H = 1$. In the sphere wall the radial stress increases for $n < 0$ and decreases for $n > 0$. The magnitude of decrease or increase of the stress depends on $|n|$. The distribution of the compressive meridional stress of the sphere along the radius is shown in Fig. 12. The value of the stress is not the same in the inner and outer layers and $\sigma_\varphi / \sigma_\varphi^H$ does not equal to one. The value of the meridional stress is more than the homogeneous material for $n < 0$ in the inner half of the wall thickness while it is less than that in the outer half. This will be reverse, where $n > 0$. The meridional stress is almost constant along the radius for $n = 1$. It is observed that in the range of the inner layer of the sphere, the graphs converge and behave similarly.

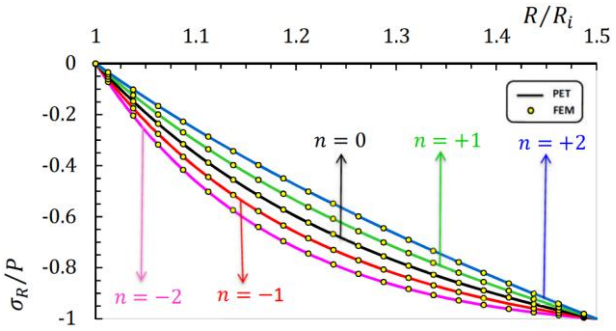

Fig. 11 Distribution of radial stress, P_o = 80 MPa (heterogeneous sphere)

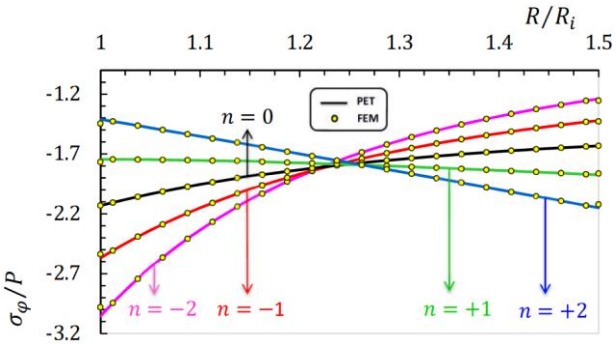

Fig. 12 Distribution of meridional stress, P_o = 80 MPa (heterogeneous sphere)

Fig. 13 shows the distribution of the radial displacement of the sphere along the wall thickness. u_R / u_R^H

does not equal one at any point. The value of the radial displacement is more than the homogeneous material for $n < 0$ while it is less than that for $n > 0$. Yet this ratio remains almost constant along the wall thickness.

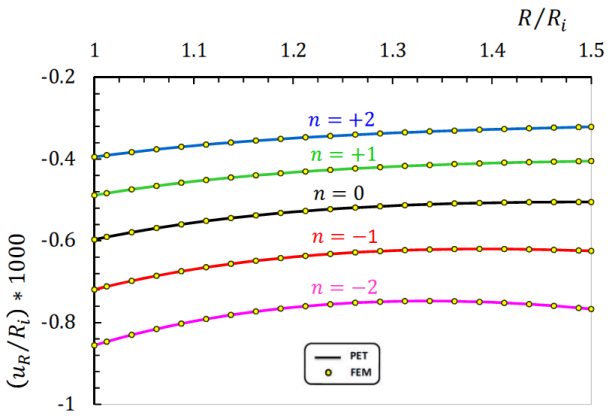

Fig. 13 Distribution of radial displacement, P_o = 80 MPa (heterogeneous sphere)

5.2.3. Internal and external pressure

The nonhomogeneous sphere is subjected to the internal and external pressures, $P_i = P_o = P$ = 80 MPa.

The distribution of the compressive radial stress of the sphere along the wall thickness is shown in Fig. 14. The value of the radial stress in the inner and outer layers of the sphere is the same and $\sigma_R / \sigma_R^H = 1$. In the sphere wall, the radial stress is more than the radial stress of the homogeneous sphere for $n < 0$ and is the reverse for $n > 0$. In the homogeneous sphere, radial stress is almost constant along the wall thickness.

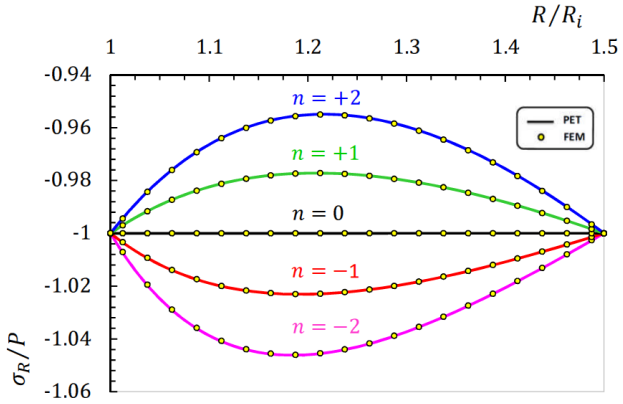

Fig. 14 Distribution of radial stress, $P_i = P_o$ = 80 MPa (heterogeneous sphere)

The distribution of the compressive meridional stress of the sphere along the wall thickness is shown in Fig. 15. The value of the meridional stress is not the same in the inner and outer layers of the sphere and $\sigma_\varphi / \sigma_\varphi^H$ does not equal to one. The value of the meridional stress is more than the homogeneous material for $n < 0$ in the inner half of the wall thickness while it is less than that in the outer half. This will be reverse, where $n > 0$. The meridional stress is almost constant along the radius for $n = 0$. It is observed that in the range of the inner layer of the sphere, the graphs converge and behave similarly. Fig. 16 shows the distribution of the radial displacement of the sphere along the wall thickness. u_R / u_R^H is not one at any point. In the sphere wall, the radial displacement is more than the radial displacement of the homogeneous sphere for $n < 0$ and is the reverse for $n > 0$. In the homogeneous sphere, radial displacement is almost constant along the wall thickness.

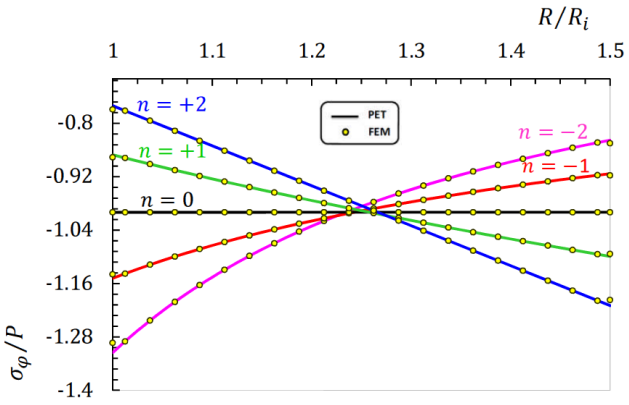

Fig. 15 Distribution of meridional stress, $P_i = P_o$ = 80 MPa (heterogeneous sphere)

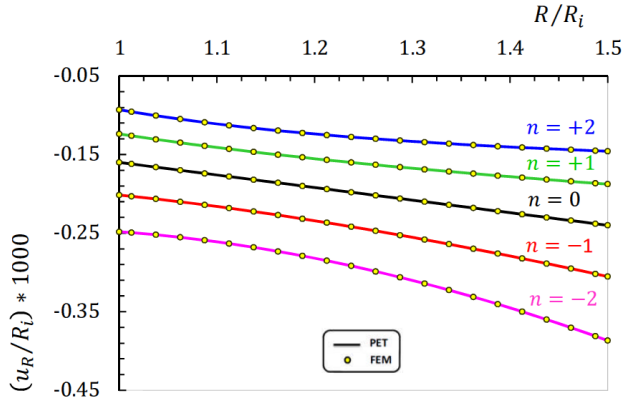

Fig. 16 Distribution of radial displacement, $P_i = P_o$ = 80 MPa (heterogeneous sphere)

In Table, the values of effective stress resulting from analysis of sphere through PET and FEM under internal pressure and/or external pressure in the middle layer are given.

Table

Comparison of values of effective stress resulting from PET and FEM in the middle layer

		$n = -2$	$n = -1$	$n = 0$	$n = +1$	$n = +2$
P_i = 80 MPa	PET	77.81	82.90	87.31	90.88	93.51
	FEM	77.95	83.01	87.39	90.92	93.53
P_o = 80 MPa	PET	73.31	80.89	87.31	92.35	95.85
	FEM	73.48	81.01	87.39	92.38	95.86
$P_i = P_o$ = 80 MPa	PET	4.50	2.02	0	1.47	2.34
	FEM	4.47	2.00	0	1.46	2.33

6. Conclusions

It can be concluded that for both positive and negative values of *n*, the meridional stress in the nonhomogeneous sphere decreases in one half and increases in the other. In the nonhomogeneous sphere compared to the homogeneous one, with no external pressure, the radial stress increases and the radial displacement decreases for positive *n*. For negative *n* both radial stress and radial displacement increase in the spheres subjected to external pressure. The radial stress and radial displacement decrease for positive *n.* Decrease or increase of the radial stress and radial displacement depend on |*n*|. According to the requirements for decreasing of the displacement and stress in the nonhomogeneous spheres, the positive or negative values of *n* could be applied.

References

1. **Timoshenko, S.P.; Goodier, J.N.** 1970. Theory of Elasticity, 3rd Edition, New York: McGraw-Hill, 395p.
2. **Tutuncu, N.; Ozturk, M.** 2001. Exact solutions for stresses in functionally graded pressure vessels, Composites Part B-Engineering 32(8): 683-686. http://dx.doi.org/10.1016/S1359-8368(01)00041-5.
3. **You, L.H.; Zhang, J.J.; You, X.Y.** 2005. Elastic analysis of internally pressurized thick-walled spherical pressure vessels of functionally graded materials, International Journal of Pressure Vessels and Piping 82(5): 347-354. http://dx.doi.org/10.1016/j.ijpvp.2004.11.001.
4. **Chen, Y.Z.; Lin, X.Y.** 2008. Elastic analysis for thick cylinders and spherical pressure vessels made of functionally graded materials, Computational Materials Science 44(2): 581-587. http://dx.doi.org/10.1016/j.commatsci.2008.04.018.
5. **Li, X-F.; Peng, X-L.; Kang, Y-A.** 2009. Pressurized hollow spherical vessels with arbitrary radial nonhomogeneity, AIAA Journal 47(9): 2262-2265. http://dx.doi.org/10.2514/1.41995.
6. **Tutuncu, N.; Temel, B.** 2009. A novel approach to stress analysis of pressurized FGM cylinders, disks and spheres, Composite Structures 91(3): 385-390. http://dx.doi.org/10.1016/j.compstruct.2009.06.009.
7. **Nejad, M.Z.; Rahimi, G.H.; Ghannad, M.** 2009. Set of field equations for thick shell of revolution made of functionally graded materials in curvilinear coordinate system, Mechanika 3(77): 18-26.
8. **Borisov, A.V.** 2010. Elastic analysis of multilayered thick-walled spheres under external load, Mechanika 4(84): 28-32.
9. **Nie, G.J.; Zhong, Z.; Batra, R.C.** 2011. Material tailoring for functionally graded hollow cylinders and spheres, Composites Science and Technology 71(5): 666-673. http://dx.doi.org/10.1016/j.compscitech.2011.01.009.

Mehdi Ghannad, Mohammad Zamani Nejad

NEVIENALYČIO HETEROGENINIO STORASIENIO KEVALO IŠSAMUS UŽDAROS FORMOS SPRENDIMAS

R e z i u m ė

Remiantis plokštumos tamprumo teorija, yra sudarytos asimetrinio storasienio sferinio kevalo, pagaminto iš nehomogeninės aukštos kokybės medžiagos, apkraunamos vidiniu ir išoriniu slėgiu, bendrosios svarbiausios lygtys. Laikoma, kad tamprumo modulis kinta netiesiškai radialine kryptimi, o Puasono koeficientas yra pastovus. Yra sudarytos realių, sudvejintų ir kompleksinių šaknų analitinio sprendimo lygtys. Radialiniai ir meridianiniai įtempiai bei radialinių poslinkių pasiskirstymas priklausomai nuo nehomogeniškumo konstantų yra palyginti su homogeniškų atveju gautais dydžiais, taip pat su baigtinių elementų metodo rezultatais ir parodyti grafikuose. Gauti rezultatai rodo, kad aukštos kokybės medžiagos savybės turi didelę įtaką įtempių pasiskirstymui radialine kryptimi. Jie yra naudingi inžinieriams, projektuojantiems sferas iš aukštos kokybės medžiagų.

Mehdi Ghannad, Mohammad Zamani Nejad

COMPLETE CLOSED-FORM SOLUTION FOR PRESSURIZED HETEROGENEOUS THICK SPHERICAL SHELLS

S u m m a r y

On the basis of plane elasticity theory (PET), the governing equations for axisymmetric thick spherical shells made of nonhomogeneous functionally graded materials (FGMs) subjected to internal and external pressure in general case are derived. It is assumed that the modulus of elasticity varies nonlinearly in the radial direction, and the Poisson's ratio is constant. The analytical solution of the equations for real, double and complex roots are obtained. The radial stress, meridional stress and radial displacement distributions depending on an inhomogeneity constant are compared with those of the homogeneous case as well as with the solution using finite element method (FEM) and presented in the form of graphs. The obtained result shows that the property of FGMs has a significant influence to the stress distribution along the radial direction. Results are useful for engineers to design a sphere made of FGMs.

Keywords: pressurized heterogeneous thick spherical shells, plane elasticity theory.

Received May 30, 2011
Accepted October 12, 2012